Hindawi
Advances in Civil Engineering
Volume 2023, Article ID 9064303, 10 pages
https://doi.org/10.1155/2023/9064303

Research Article

Modeling the Influence of Ground-Granulated Blast Furnace Slag on Hydration of Cement

Andualem Yadeta,[1,2] **Pradeep Goyal**,[1] **and Raju Sarkar**[1]

[1]*Department of Civil Engineering, Delhi Technological University, Delhi 110042, India*
[2]*Department of Construction Technology and Management, Madda Walabu University, Bale Robe 242, Ethiopia*

Correspondence should be addressed to Andualem Yadeta; andu1781@gmail.com

Received 22 April 2023; Revised 6 September 2023; Accepted 27 September 2023; Published 19 October 2023

Academic Editor: Heng-Long Zhang

Portland cement is usually substituted with granulated blast furnace slag to make a slag-blended cement. A slag-incorporating cement has a more complicated hydration process than Portland cement due to the interactions between the slag reaction and the hydration of Portland cement in the cementitious systems. Understanding the effect of slag substitution on the hydration of cement is still challenging; hence, this research is aimed at predicting the hydration of slag-incorporating cement. To achieve this, the extended CEMHYD3D model was employed to predict the hydration of a slag-blended cement. The simulation was done with cement paste samples made with various water-to-cement ratios and different slag substitution levels, in which the interaction between the hydration of Portland cement and the reaction of slag was considered. The prediction model has been validated with experimental results and verified to be successful in predicting the hydration of slag-blended cement.

1. Introduction

Supplementary cementitious materials (SCMs) such as ground-granulated blast furnace slag, often called slag cement, fly ash (FA), and silica fume (SF) are widely used in the cementitious composites due to their durability, environmental friendliness, and minimal cost. When added to Portland cement, SCMs improve the characteristics of a cementitious material via either their pozzolanic activity and/or hydraulic activity. They reduce the energy used and the CO_2 released while producing Portland cement [1], and they are widely used in cement-based composites. When compared to the composites made only with Portland cement, composites incorporating SCMs have better durability regarding several deterioration processes, such as chloride penetration and sulfate attack [2]. Slag is among the most frequently used SCMs and is made from iron blast-furnace slag during the reduction of iron ore with coke at a temperature of about 1,500°C. Slag shows high activity during hydration and comprises over 90% of glass because of quick water quenching [3]. Studies conducted by Choi et al. [4], Lee et al. [5], and Cahyani and Rusdianto [6] explained that the substitution of slag for Portland cement enhances the workability and hydration of the process.

At the microscale level, cement particles are typically made up of tricalcium silicate (C_3S), dicalcium silicate (C_2S), tricalcium aluminate (C_3A), and tetra-calcium aluminate ferrite (C_4AF) mineral phases. Cementitious materials require a supply of water for hydration, and moisture exchange can shift the water balance within the material. The volume of water in the component changes due to these two processes. Hydration is highly sensitive to the water-to-cement (w/c) ratio of the cementitious system immediately after it has been prepared. Once the cement and water are mixed, a number of chemical reactions can be performed: C_3S and C_2S produce calcium hydroxide (CH) and calcium–silicate–hydrates (C—S—H), while C_3A and C_4AF in the hydration process contribute to the formation of C_3AH_6 and FH_3 [7].

The substitution of slag for Portland cement can alter the rate of hydration and the microstructural properties of the cementitious materials. The effect of slag on the hydration of cement has been experimentally studied by Kolani et al. [3], Binici et al. [8], and Zhao et al. [9]. In other studies, advanced characterization methods like scanning electron microscopy (SEM) [10] and X-ray diffraction (XRD) [11] were employed to determine the hydration and microstructure of various

blended cements. But techniques like SEM and XRD analysis can also be time-consuming and costly. Computer models are helpful to simulate the hydration of cement. As long as water and space are available, the volume of cement and hydration change over time and continue to do so during the hydration process. Computer models simulate these changes using volume stoichiometries based on the material properties. On the basis of hydration models for cementitious systems that use solely Portland cement, a number of computer-based models such as CEMHYD3D [12], HYMOSTRUC3D [13, 14], μic [15], and DuCOM [16] were developed to predict the hydration of cement and how its microstructure changes over time. Several multiscale models for the hydration of Portland cement have been developed and are now in use throughout the last few decades [17–19]. The existing models of hydration were developed to predict the hydration of composites made of only Portland cement. The rate of hydration in a single cement system was predicted previously by Park [20], in which the rate of hydration that results from the free water reduction and reduced interaction area within the hydration products was considered. The hydration of cements incorporating SCMs like slag is more complex than that of cementitious systems involving only Portland cement owing to the mineral reactions involved in SCMs. The mineral reactions during the hydration of cements involving SCMs such as slag, FA, and limestone are considered distinct from those involving regular Portland cement, and some reactions are considered by looking at the concentration of calcium hydroxide and free water.

A general hydration model was developed by Maekawa et al. [16] for concrete containing FA and slag. A hydration model for limestone containing cement was developed and validated by Mohamed et al. [21]. As described by Swaddiwudhipong et al. [22], the study predicted the hydration of cements containing SF in concrete with a computer model. A multiphase hydration model was proposed by Merzouki et al. [19] and Meinhard and Lackner [23]. The heat generation and the various microstructural characteristics of slag-incorporating cement are all dependent on the hydration of the minerals involved in each cement in the composite. However, there are currently no models available to predict the rate of hydration of slag-incorporating cements. Furthermore, the prediction models that were developed in the previous studies did not consider how slag influences the rate of hydration of a cement system, considering the w/c ratio and the slag replacement level in the system. Therefore, there is a need to consistently predict the hydration of slag-incorporating cementitious systems with the computer models.

2. Hydration Modeling

A modeling software called CEMHYD3D was created for the first time by the National Institute of Standards and Technology to describe the hydration and microstructure of cement [12]. In this model, the microstructure is explained as a grid of volume pixels, each of which stands for a different type of hydration phase. CEMHYD3D is an effective tool for simulating cement hydration that can also involve SCMs [24]. Because the model simulates the cement particles based on actual cement pictures and particle size distributions, it can accurately model the compositions of cement particles and distributions of phases. So, the extended CEMHYD3D version 3.0 modeling package is proposed to predict the hydration of slag-incorporating cements in this study.

2.1. Hydration Model for Portland Cement. The hydration of a single cement particle can be calculated using the basic equation expressed in Equation (1) for each chemical composition in the cement [25]. The activation of chemical reaction and the diffusion process during hydration of a single cement are all taken into account in this model:

$$\frac{d\alpha}{\mathrm{dt}} = \left[\frac{3\left(\frac{S_w}{S_0}\right)\rho_w C_{w\text{-}fre}}{\left(v + w_g\right) r_0 \rho_c}\right] x \left[\frac{1}{\left(\frac{1}{k_d} - \frac{r_0}{D_e}\right) + \frac{r_0}{D_e}(1-\alpha)^{\frac{-1}{3}} + \frac{1}{k_r}(1-\alpha)^{\frac{-2}{3}}}\right], \tag{1}$$

where α is the degree of hydration of cement, v is the mass ratio of water to cement, w_g is the physically bound water in the C—S—H gel, S_w is the effective surface area of the cement particles that are in contact with water, S_0 is the total surface area, $C_{w\text{-}fre}$ is the physically free water in the C—S—H gel, r_0 is the radii of an unhydrated cement particle, ρ_c is the density of cement, and ρ_w is the density of water, k_d is the reaction coefficient in the dormant period, k_r is the coefficient of the rate of reaction for each mineral, and D_e is the effective diffusion coefficient of water in the hydration products for each mineral constituents.

The reaction coefficient, k_d in Equation (2) is assumed to be proportional to the rate of hydration of cement, whereas the values of coefficients B and C govern the initial rates of shell formation and decay, respectively.

$$k_d = \frac{B}{\alpha^{1.5}} + C\alpha^3. \tag{2}$$

In regard to hydrates, the effective diffusion coefficient of water changes based on the radii of the gel pore in the cementitious system. The following Equation (3) presents an expression for this phenomenon in terms of the rate of hydration.

$$D_{e0} = \ln\left(\frac{1}{\alpha}\right). \tag{3}$$

Moreover, when the hydration of the minerals in each cement continues, the free water in the capillary pores reduces. Therefore, it is important to consider that some amount of water can be trapped in the gel pores and may be used for further hydration at every stage of hydration [20]. Hence, as shown in Equation (4), the amount of water in the capillary pore varies with the rate of hydration.

Table 1: Reaction of slag [33].

Quantity measured	Values (g/g of slag)
Calcium hydroxide	0.22
Chemically bound water	0.30
Gel water	0.15

$$C_{w\text{-}free} = \frac{W_0 - 0.4\alpha C_0}{W_0}, \quad (4)$$

where C_0 and W_0 represent the initial percentages by mass of cement and water in the mixture.

Hydration modeling covers the chemical effects of the cement minerals in the hydration reactions. According to the theories put forth by Papadakis [26], Lu et al. [27], and Maciel et al. [28], the reactions that the minerals in Portland cement undergo during the hydration stage can be described with Equations (5)–(8) as follows:

$$2C_3S + 6H \rightarrow C_3S_2H_3 + 3\text{CH}, \quad (5)$$

$$2C_2S + 4H \rightarrow C_3S_2H_3 + \text{CH}, \quad (6)$$

$$C_3A + C\overline{S}H_2 \rightarrow 10H + C_4\text{A}\overline{S}\overline{H}_{12}, \quad (7)$$

$$C_4\text{AF} + 2\text{CH} \rightarrow 10H + C_6\text{AFH}_{12}. \quad (8)$$

Both CH and C—S—H are formed when C_3S and C_2S are hydrated with water. As long as C_3A or C_4AF aluminate clinker phases are present, aluminate is absorbed by C—S—H which produces a C—A—S—H product. If no remaining aluminate reactants are left, the C_3S and C_2S reactions further yield CSH without aluminum substitution. However, using Equations (5)–(8), the mass per volume of the CH and C—S—H products in Portland cement can be calculated.

2.2. Hydration Model for Slag-Incorporating Cement. There are five major hydration products that occur when slag is added to cement: C—S—H, C—S—A—H, hydrotalcite (M_5AH_{13}), ettringite ($C_6A\overline{S}_3H_{32}$), and AFm phase (C_4AH_{13}) are usually formed [29]. While both slag and Portland cement produce similar hydration products, part of the portlandite produced when cement clinker hydrates is actually consumed when slag is hydrated [30–32]. Nevertheless, a high rate of slag reaction requires a lower w/c ratio [26]. The reaction of slag during hydration is appropriately summarized by the approximate critical values shown in Table 1, as reported by Maekawa et al. [33], based on his study conducted on the blended cements.

In accordance with the stoichiometry and hydration model of the slag reaction [33], the mass of calcium hydroxide, the chemically bound water, and the gel water may all be computed with Equations (9)–(11) in which the hydration of slag-incorporating cements can be described as follows:

$$\text{CH} = \text{RCH}_{\text{ce}}\, xC_0x\alpha - \text{RCH}_{\text{sg}}x\alpha_{\text{sg}}xP, \quad (9)$$

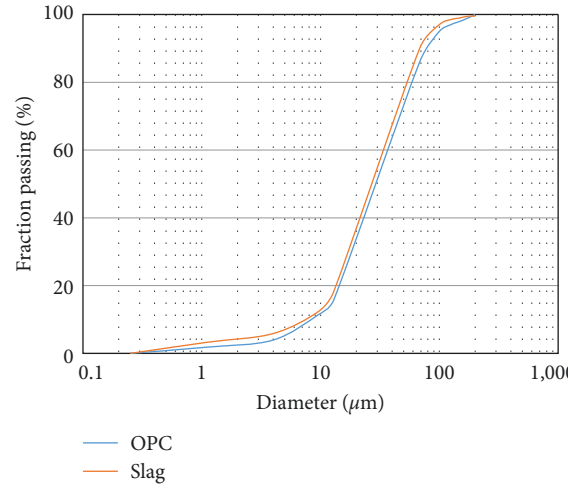

Figure 1: Particle size distribution of OPC and slag used in the model.

$$W_{\text{cap}} = W_0 - 0.4xC_0x\alpha - \text{RCW}_{\text{sg}}\, x\alpha_{\text{sg}}\text{xP} - \text{RPW}_{\text{sg}}x\alpha_{\text{sg}}xP, \quad (10)$$

$$W_{\text{cbw}} = vxC_0x\alpha + \text{RCW}_{\text{sg}}x\alpha_{\text{sg}}xP, \quad (11)$$

where CH, W_{cap}, and W_{cbw} are the mass of calcium hydroxide, capillary water, and chemically bound water, respectively. sg is the rate of the slag reaction, P is the mass of the slag in the mix, RCH_{ce} and RCH_{sg} are the mass of calcium hydroxide formed in the hydration of cement, and the slag reaction in that order, where as RCW_{sg} and RPW_{sg} are the mass of chemically bound water and the gel water in the slag reaction, respectively.

3. Experiments

An OPC as a reference cement confirmed to ASTM C 150 and a slag confirmed to ASTM C 989 standard requirements were used in this study. Before the simulation of the rate of hydration of slag-incorporating cement with the proposed model, the individual cements were first characterized according to their particle size distribution (PSD) and chemical compositions. The average PSD for OPC and slag was measured with a laser diffraction (LD) technique and plotted in Figure 1. The hydration model development needs the consideration of some reaction chemistry, for which standard abbreviations are used throughout the model: C stands for CaO, S for SiO_2, A for Al_2O_3, F for Fe_2O_3, M for MgO, and H for H_2O. The hydration equations of the four cement clinker phases (C_3S, C_2S, C_3A, and C_4AF) and slag reactions are considered in the model.

As a reference cement, an OPC with the chemical composition presented in Table 2 is used to determine the influence of the substitution of slag into cement. While simulating the hydration of the blended cement, the w/c ratio and the slag replacement level were considered.

The proposed CEMHYD3D model from open source offers the possibility of simulating the hydration of cement.

Table 2: Chemical composition of the OPC used in the model (mass%).

Clinker phase	Volume fraction	Surface area fraction
C_3S	0.7229	0.6689
C_2S	0.0961	0.1377
C_3A	0.1291	0.1346
C_4AF	0.0397	0.0391

Table 3: Compound composition of the slag used in the model (mass%).

SiO_2 (%)	CaO (%)	Al_2O_3 (%)	SO_3 (%)	MgO (%)	Fe_2O_3 (%)	K_2O (%)	Na_2O (%)
40.23	35.04	11.18	6.80	2.32	2.05	0.43	0.29

Moreover, the code in the program allows us to adjust the model for extension as necessary.

To extend the CEMHYD3D model and enhance its predictive capabilities, a critical refinement has been introduced by incorporating the reaction of slag into the program. This significant modification is applied because the rate of hydration in cementitious systems is intricately linked to the mineral composition of each specific type of cement.

The compound composition of the slag used in the model is presented in Table 3. In a slag-blended cement system, the simplest and most direct approach is to assume that the slag reacts with CH in the hydration process and yields a single product with a mixed phase. This process provides a C—S—H product that has a lower ratio of Ca/Si than the typical C—S—H product, amorphous silica (AFm), and some hydrotalcite products [34, 35].

Various samples of cement pastes were prepared with a w/c ratio of 0.3, 0.4, 0.5, and 0.6 at a slag replacement level of 10%, 20%, 30%, and 40% by mass of cement. The pastes were made by mixing the raw materials in a vertical axis pot mixer with water first, then slowly adding cementitious materials while the blades were rotating; the subsequent mixing process included a 3-min low speed mixing, a half-minute pause, and a 2-min high speed mixing. After being mixed, fresh mixtures were cast into plastic tubes of φ15 mm, and the two ends of the tubes were sealed to prevent moisture exchange. The sealed specimens were cured in a saturated condition at a standard temperature of 20°C until the age of testing. The specimens were tested at specific ages of 1, 3, 7, 28, and 90 days. The contents of hydrate water and CH in the Portland cement and blended cement pastes were determined using thermogravimetric analysis (TGA). The specimens were removed from the plastic tubes, ground to a fine powder with particles of size $<60\,\mu$m in a chamber, and flushed with methanol in a thistle tube connected to a vacuum to arrest the hydration. After drying, about 40 mg of the powder sample was analyzed by measuring the weight while heating the sample up from standard temperature to 550°C in TGA. Weight loss in the ranges of 450–550°C was used to compute the contents of hydrate water and CH, respectively [36–38]. The amount of hydrate water per gram of binder (w_H) was calculated by normalizing the hydrate water content by the mass loss of the sample between 450–550°C divided by the mass of the ignited sample, corrected for the measured loss-on-ignition of the unhydrated cement (or of the unhydrated cement divided by the percentage of slag for slag-blended cement). The values of w_H were converted to estimated degrees of hydration (α) based on the phase composition of the cement used in the study.

4. Simulation of the Influence of Slag on Hydration of Cement

Cement pastes with various values of w/c and replacement levels of OPC with slag were created using the extended CEMHYD3D version model to match the experimental mix. In all simulations of the proposed cement paste, a conversion factor of 0.00035 hr/cycle^2 as described by Bentz [12] has been applied to make conversions between the model hydration cycles and the real time. As discussed in previous sections, it was assumed in this study that the slag in a blended cement reacts with CH and provides a single product of hydration in a mixed phase. With the proposed model, the hydration of slag-incorporating cement was simulated using cement paste samples made with a replacement level of 10%, 20%, 30%, and 40% by mass of slag and a w/c of 0.3, 0.4, 0.5, and 0.6. The prediction has been validated with measured values from experiments based on the standard test method of ASTM C186. Previously, experimental studies were conducted by Zhao et al. [9], Durdziński et al. [39], and Hlobil et al. [40]. In slag-incorporating cement, the amount of CH and the rate of reaction of mineral components determine the rate of hydration of the cement [3, 9]. This proves that the hydration product of slag usually develops in close proximity to the slag particles [41–43]. Using the approach suggested by Saeki and Monteiro [44], the equation for the reaction of slag can be expressed with Equations (12)–(14) as follows, considering the aforementioned factors:

$$\frac{d\alpha_{sg}}{dt} = \left(\frac{m_{CH}(t)}{P}\right)\left(\frac{W_{cap}}{W_0}\right)\left(\frac{3P_W}{\nu_{sg} r_{sgo} \rho_{sg}}\right) x \frac{1}{\left(\frac{1}{k_{dsg}} - \frac{r_{SO0}}{D_{esg}}\right)\left(1-\alpha_{sg}\right)^{-\frac{1}{3}} + \left(\frac{1}{k_{rsg}}\right)\left(1-\alpha_{sg}\right)^{-\frac{2}{3}}}, \quad (12)$$

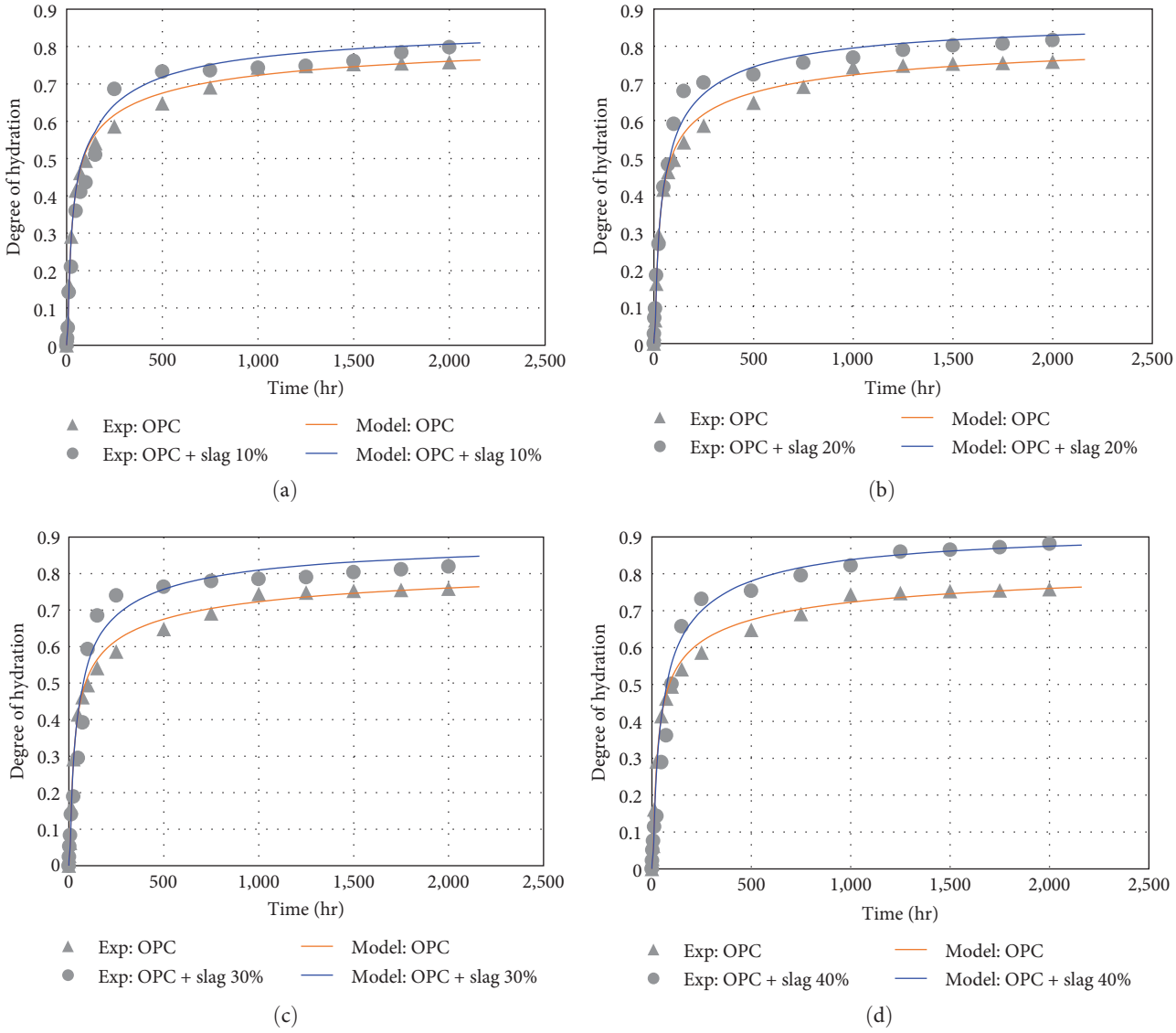

FIGURE 2: Simulated degree of hydration of cement with different % by mass slag substitution for w/c = 0.3. (a) Cement paste without and with 10% slag. (b) Cement paste without and with 20% slag. (c) Cement paste without and with 30% slag. (d) Cement paste without and with 40% slag.

$$k_{dsg} = \frac{B_{sg}}{(\alpha_{sg})^{1.5}} + C_{sg}(\alpha_{sg})^3, \tag{13}$$

$$D_{esg} = D_{esg0} x \ln\left(\frac{1}{\alpha_{sg}}\right), \tag{14}$$

where $m_{CH}(t)$ is the mass of calcium hydroxide formed in the hydrated slag-blended mixes obtained from Equation (9), D_{esg0} is the initial diffusion coefficient, ρ_{sg} is the density of slag, k_{dsg} is the rate of reaction coefficient of slag in the dormant phase (B_{sg} and C_{sg} are coefficients), and k_{rsg} is the rate of reaction coefficient of slag.

5. Analysis and Discussion

Figures 2–5 shows the hydration of slag-incorporated cements, which were simulated with the extended CEMHYD3D model for different w/c values and various replacement levels. The simulations with the computer model were carried out under the same conditions as the experiments. The model provided a good prediction of the influence of slag on the hydration of cement in all simulations, which agreed with the experimental results.

The hydration of slag-incorporated cement is simulated in Figure 2 separately as a, b, c, and d in volume fractions of each cement. The model predicted the hydration of blended cement pastes without and with 10%, 20%, 30%, and 40% slag substitution made with a w/c of 0.3 for all mixes under sealed conditions at a temperature of 20°C. It was observed

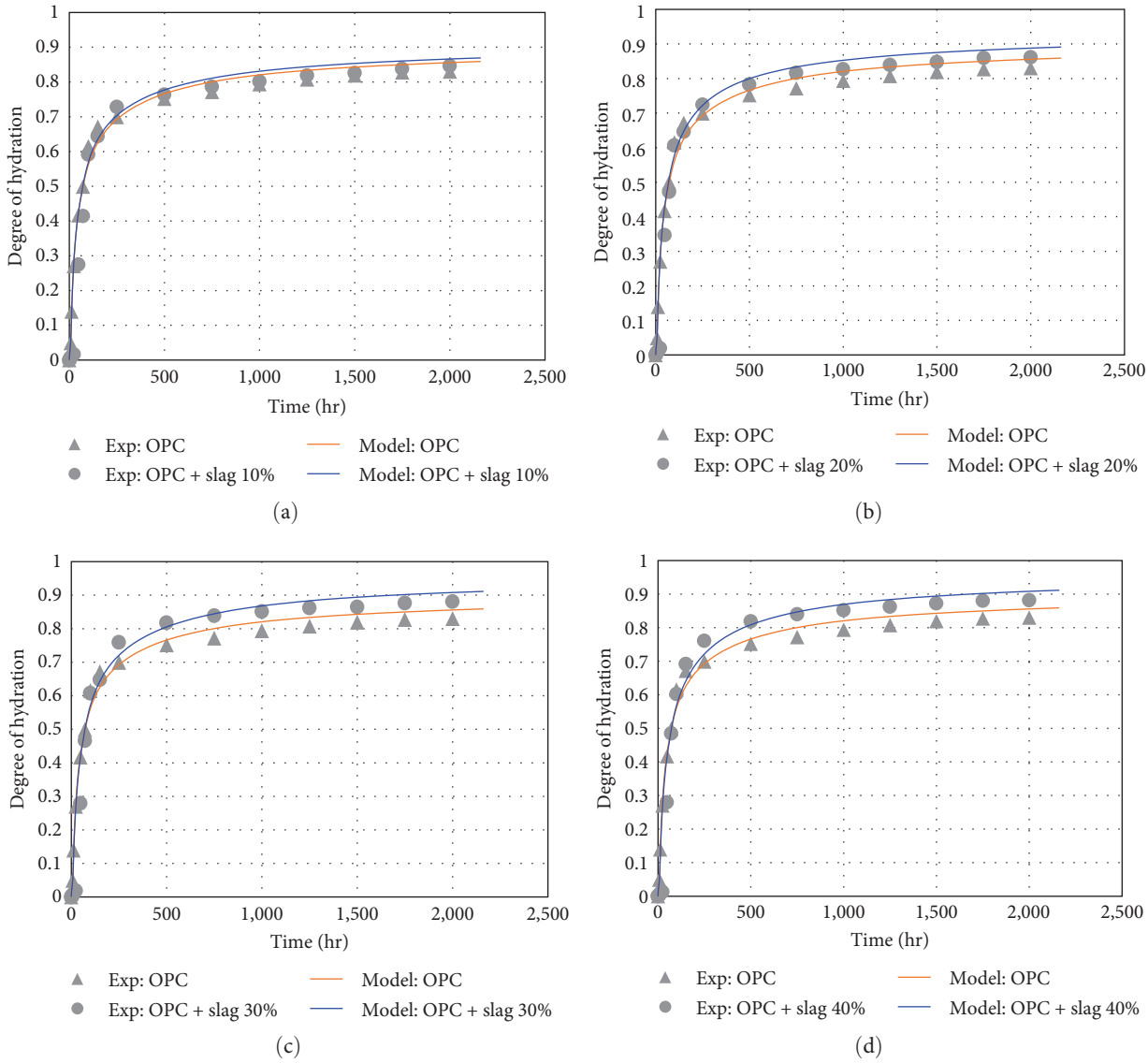

FIGURE 3: Simulated degree of hydration of cement with different % by mass slag substitution for w/c = 0.4. (a) Cement paste without and with 10% slag. (b) Cement paste without and with 20% slag. (c) Cement paste without and with 30% slag. (d) Cement paste without and with 40% slag.

that the cement clinker phase reacted much faster than the reaction of slag in the early ages. Slag can significantly reduce the heat needed for hydration when substituted for cement [45]. However, the slag continues to react at a later age while the clicker phase reaction decreases. In all mixes, the slag reaction increases as the substitution percentage of slag increases, and it was observed that the rate of hydration at a later age increases when a lower w/c of about 0.3 is used in the mix.

As shown in Figure 3 below, the model predicted the influence of slag on the rate of hydration of cement for pastes without and with 10%, 20%, 30%, and 40% slag substitution for a w/c of 0.4 for all mixes under sealed conditions at 20°C. The prediction indicated that no substantial effect of slag on the rate of hydration of cement was observed when up to 10% slag was substituted for a w/c of 0.4. Even though the reaction of clicker phases in the early age is faster than the reaction of slag, the simulation illustrates that the hydration of the blend increases as the substitution level of slag into cement increases in the later age, when a w/c of about 0.4 is used for the paste.

The prediction in a, b, c, and d of Figure 4 illustrates that the rate of reaction of slag at a replacement level of 10%, 20%, 30%, and 40% is similar in most cases with the paste with 0% slag cement when a w/c of 0.5 is utilized for the mix. From the model prediction, no significant effect was observed between the hydration of Portland cement and a slag-incorporating cement in the early ages, when about 10% slag was substituted. In contrast, using a w/c of 0.5 accelerates the rate of hydration in the later age at about 90 days and increases as the substitution percentages of slag in the blend increase.

The predicted values for hydration of a slag-blended cement made with a w/c of 0.6 and varying slag substitution

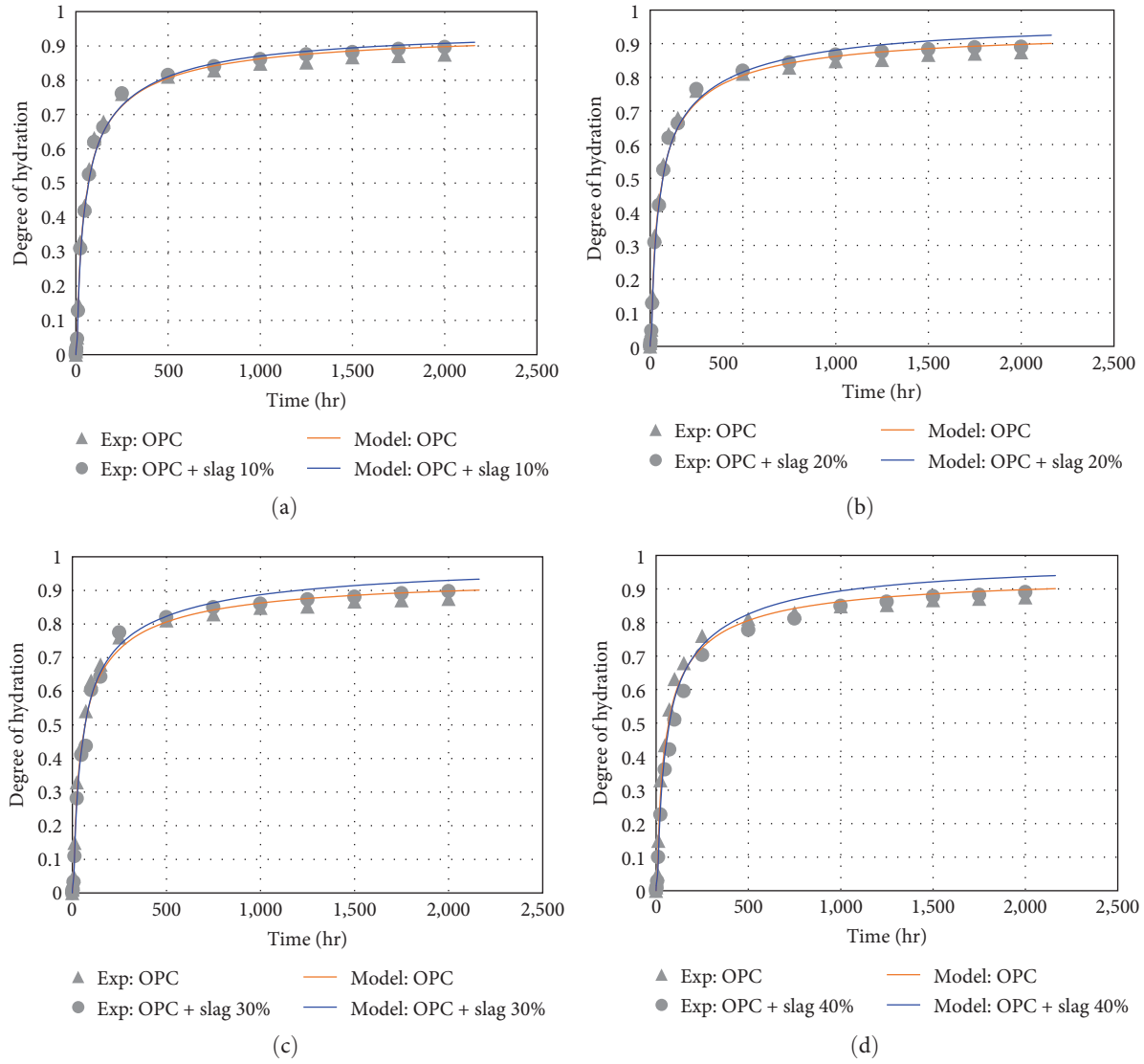

FIGURE 4: Simulated degree of hydration of cement with different % by mass slag substitution for w/c = 0.5. (a) Cement paste without and with 10% slag. (b) Cement paste without and with 20% slag. (c) Cement paste without and with 30% slag. (d) Cement paste without and with 40% slag.

levels are also plotted in a, b, c, and d of Figure 5. The rate of hydration of Portland cement and up to 10% by mass slag substituted cement paste is similar when w/c is around 0.6. When compared with the clicker phase, the reaction of slag slightly increases as the slag substitution level increases, even at the later age of 90 days when the same w/c is used in both mixes.

The hydration of a slag-incorporating cement was accurately predicted using the extended CEMHYD3D model. The hydration of cement pastes made with a w/c ratio of 0.3, 0.4, 0.5, and 0.6 and with a slag replacement level of 10%, 20%, 30%, and 40% was simulated for the age of 90 days cured in a saturated condition at a standard temperature of 20°C. The model prediction and the measured values from experiments were in good agreement in all mixes. The simulation shows that the slag-incorporating cement was predicted to have greater hydration than the Portland cement in the later ages. The rate of hydration of the blend with slag is found to be higher for a w/c of 0.3 and negligible when a w/c of about 0.6 is used. Hence, a greater slag reaction for hydration is preferred at a higher w/c. This makes sense given that there is more space and water in the paste available for reactions and the formation of products. Moreover, there is more water accessible for cement hydration at the paste level. The simulation clearly shows that the rate of reaction of the slag in the blend increases proportionally as the slag substitution level increases. According to Ahmad et al. [46], when the fraction of slag is increased up to 60% in cement, it reduces the amount of time required to reach a maximal rate of hydration. However, no substantial change was observed in the rate of hydration for a slag substitution up to 10% in Portland cement.

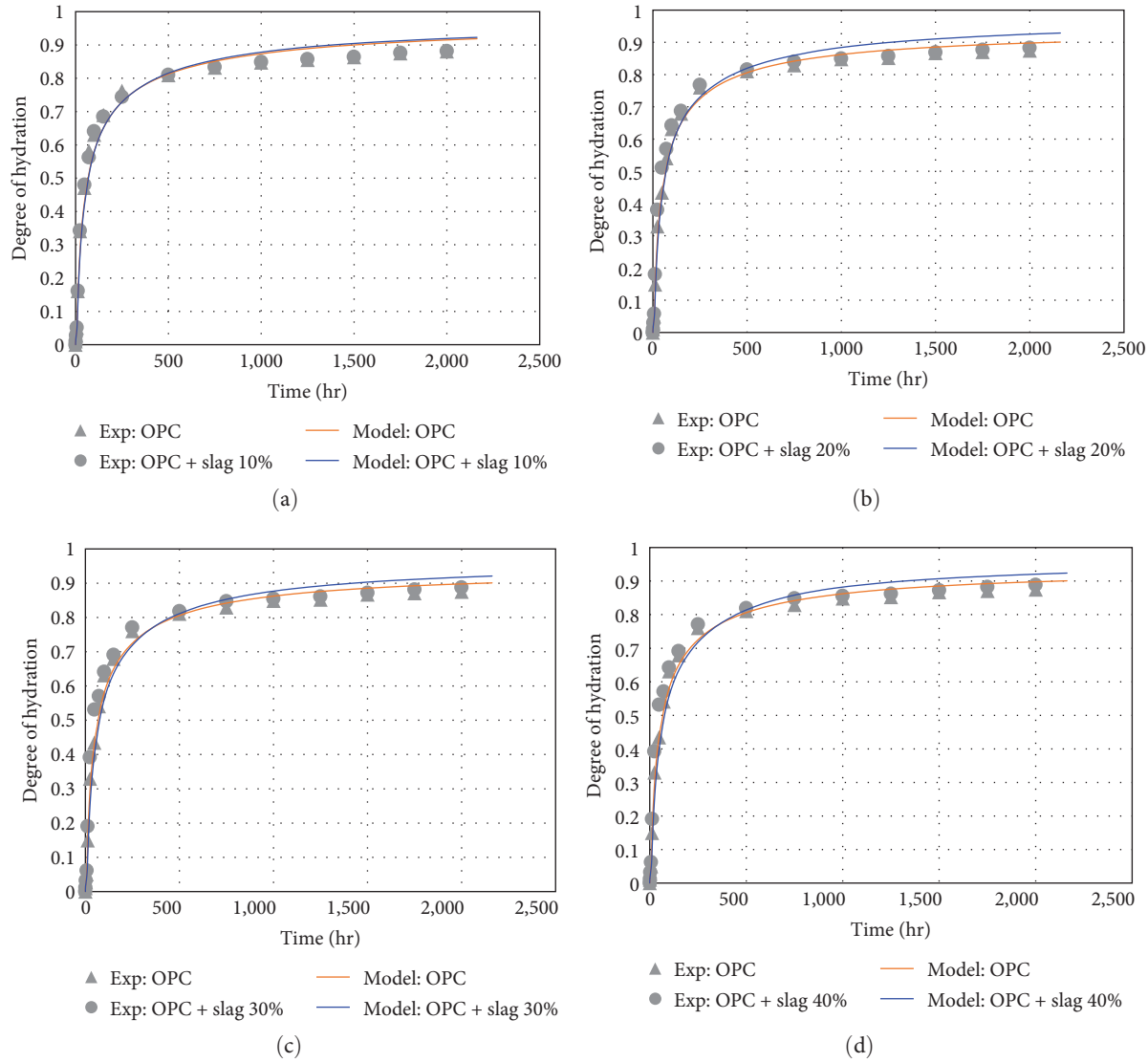

FIGURE 5: Simulated degree of hydration of cement with different % by mass slag substitution for w/c = 0.6. (a) Cement paste without and with 10% slag. (b) Cement paste without and with 20% slag. (c) Cement paste without and with 30% slag. (d) Cement paste without and with 40% slag.

6. Conclusions

The paper presented the simulation of the influence of slag substitution on the hydration of cement using the extended CEMHYD3D version 3.0 model. The model predictions agreed with the experimental values regarding the w/c ratio and substitution percentage of slag in Portland cement. The possible influence of slag on the hydration of cement is higher when a lower w/c of about 0.3 is used in the mixture in the later ages as the replacement level of slag increases. The increase in w/c ratio to about 0.6 can accelerate the early hydration of slag-blended cement systems but it has a negligible effect in the later ages as the replacement level of slag increases. Thus, slag substitution in Portland cement is recommended with a higher w/c ratio to achieve an optimal hydration result. The rate of slag reaction in a blended cement system is variable and dependent on the substitution level of the slag. The consideration of the chemical composition of slag improves the predictability of hydration in cement, and the same method was applied in this model. Both in the early age and up to the age of 90 days, the hydration of slag-incorporating cement can be predicted with the proposed model.

Data Availability

The data supporting the findings of this study are available from the corresponding author upon request.

Conflicts of Interest

The authors declare that they have no conflicts of interest.

Acknowledgments

This study was supported by Ministry of Education of the Federal Democratic Republic of Ethiopia.

References

[1] D. Wang, X. Zhou, Y. Meng, and Z. Chen, "Durability of concrete containing fly ash and silica fume against combined freezing-thawing and sulfate attack," *Construction and Building Materials*, vol. 147, pp. 398–406, 2017.

[2] S.-W. Yoo and S.-J. Kwon, "Effects of cold joint and loading conditions on chloride diffusion in concrete containing GGBFS," *Construction and Building Materials*, vol. 115, pp. 247–255, 2016.

[3] B. Kolani, L. Buffo-Lacarrière, A. Sellier, G. Escadeillas, L. Boutillon, and L. Linger, "Hydration of slag-blended cements," *Cement and Concrete Composites*, vol. 34, no. 9, pp. 1009–1018, 2012.

[4] Y. C. Choi, J. Kim, and S. Choi, "Mercury intrusion porosimetry characterization of micropore structures of high-strength cement pastes incorporating high volume ground granulated blast-furnace slag," *Construction and Building Materials*, vol. 137, pp. 96–103, 2017.

[5] J.-Y. Lee, J.-S. Choi, T.-F. Yuan, Y.-S. Yoon, and D. Mitchell, "Comparing properties of concrete containing electric arc furnace slag and granulated blast furnace slag," *Materials*, vol. 12, no. 9, Article ID 1371, 2019.

[6] R. A. T. Cahyani and Y. Rusdianto, "Concrete performance with ground granulated blast furnace slag as supplementary cementitious materials," *IOP Conference Series: Materials Science and Engineering*, vol. 771, no. 1, Article ID 012062, 2020.

[7] H. Minard, S. Garrault, L. Regnaud, and A. Nonat, "Mechanisms and parameters controlling the tricalcium aluminate reactivity in the presence of gypsum," *Cement and Concrete Research*, vol. 37, no. 10, pp. 1418–1426, 2007.

[8] H. Binici, H. Temiz, and M. M. Köse, "The effect of fineness on the properties of the blended cements incorporating ground granulated blast furnace slag and ground basaltic pumice," *Construction and Building Materials*, vol. 21, no. 5, pp. 1122–1128, 2007.

[9] Y. Zhao, J. Gao, Z. Xu, S. Li, X. Luo, and G. Chen, "Long-term hydration and microstructure evolution of blended cement containing ground granulated blast furnace slag and waste clay brick," *Cement and Concrete Composites*, vol. 118, Article ID 103982, 2021.

[10] H. Zeng, S. Qu, and Y. Qin, "Microstructure and transport properties of cement-based material enhanced by graphene oxide," *Magazine of Concrete Research*, vol. 73, no. 19, pp. 1011–1024, 2021.

[11] M. Zhang, "Pore-scale modelling of relative permeability of cementitious materials using X-ray computed microtomography images," *Cement and Concrete Research*, vol. 95, pp. 18–29, 2017.

[12] D. P. Bentz, *CEMHYD3D: A Three-Dimensional Cement Hydration and Microstructure Development Modeling Package*, National Institute of Standards and Technology, Gaithersburg, MD, Version 3.0., NIST Interagency/Internal Report (NISTIR), 2005.

[13] K. Van Breugel, "Numerical simulation of hydration and microstructural development in hardening cement-based materials (I) theory," *Cement and Concrete Research*, vol. 25, no. 2, p. 319, 331, 1995.

[14] P. Gao, G. Ye, J. Wei, and Q. Yu, "Extension of the Hymostruc3D model for simulation of hydration and microstructure development of blended cements," *Heron*, vol. 64, no. 1-2, pp. 125–148, 2019.

[15] S. Bishnoi and K. L. Scrivener, "μic: A new platform for modelling the hydration of cements," *Cement and Concrete Research*, vol. 39, no. 4, pp. 266–274, 2009.

[16] K. Maekawa, T. Ishida, and T. Kishi, "Multi-scale modeling of concrete performance integrated material and structural mechanics," *Journal of Advanced Concrete Technology*, vol. 1, no. 2, pp. 91–126, 2003.

[17] J. Carette and S. Staquet, "Monitoring and modelling the early age and hardening behaviour of eco-concrete through continuous non-destructive measurements: Part I. Hydration and apparent activation energy," *Cement and Concrete Composites*, vol. 73, pp. 10–18, 2016.

[18] F. Lin and C. Meyer, "Hydration kinetics modeling of Portland cement considering the effects of curing temperature and applied pressure," *Cement and Concrete Research*, vol. 39, no. 4, pp. 255–265, 2009.

[19] T. Merzouki, M. Bouasker, N. E. H. Khalifa, and P. Mounanga, "Contribution to the modeling of hydration and chemical shrinkage of slag-blended cement at early age," *Construction and Building Materials*, vol. 44, pp. 368–380, 2013.

[20] K.-B. Park, "Prediction of temperature and moisture distributions in hardening concrete by using a hydration model," *Architectural Research*, vol. 14, no. 4, pp. 153–161, 2012.

[21] A. R. Mohamed, M. Elsalamawy, and M. Ragab, "Modeling the influence of limestone addition on cement hydration," *Alexandria Engineering Journal*, vol. 54, no. 1, pp. 1–5, 2015.

[22] S. Swaddiwudhipong, H. Wu, and M. H. Zhang, "Numerical simulation of temperature rise of high-strength concrete incorporating silica fume and superplasticiser," *Advances in Cement Research*, vol. 15, no. 4, pp. 161–169, 2003.

[23] K. Meinhard and R. Lackner, "Multi-phase hydration model for prediction of hydration-heat release of blended cements," *Cement and Concrete Research*, vol. 38, no. 6, pp. 794–802, 2008.

[24] N. Holmes, "Introducing a new cement hydration and microstructure model," *Journal of Material Science & Engineering*, vol. 7, no. 4, Article ID 1000480, 2018.

[25] J. J. Thomas, J. J. Biernacki, J. W. Bullard et al., "Modeling and simulation of cement hydration kinetics and microstructure development," *Cement and Concrete Research*, vol. 41, no. 12, pp. 1257–1278, 2011.

[26] V. G. Papadakis, "Effect of supplementary cementing materials on concrete resistance against carbonation and chloride ingress," *Cement and Concrete Research*, vol. 30, no. 2, pp. 291–299, 2000.

[27] X. Lu, Z. Ye, S. Wang, P. Du, C. Li, and X. Cheng, "Study on the preparation and properties of belite-ye'elimite-alite cement," *Construction and Building Materials*, vol. 182, pp. 399–405, 2018.

[28] M. H. Maciel, G. S. Soares, R. C. de O. Romano, and M. A. Cincotto, "Monitoring of Portland cement chemical reaction and quantification of the hydrated products by XRD and TG in function of the stoppage hydration technique," *Journal of Thermal Analysis and Calorimetry*, vol. 136, no. 3, pp. 1269–1284, 2019.

[29] W. Chen and H. J. H. Brouwers, "The hydration of slag, Part 2: reaction models for blended cement," *Journal of Materials Science*, vol. 42, no. 2, pp. 444–464, 2007.

[30] K. Luke and E. Lachowski, "Internal composition of 20-year-old fly ash and slag-blended ordinary Portland cement pastes," *Journal of the American Ceramic Society*, vol. 91, no. 12, pp. 4084–4092, 2008.

[31] R. Taylor, I. G. Richardson, and R. M. D. Brydson, "Composition and microstructure of 20-year-old ordinary Portland

cement-ground granulated blast-furnace slag blends containing 0–100% slag," *Cement and Concrete Research*, vol. 40, no. 7, pp. 971–983, 2010.

[32] J. J. Thomas, A. J. Allen, and H. M. Jennings, "Density and water content of nanoscale solid C–S–H formed in alkali-activated slag (AAS) paste and implications for chemical shrinkage," *Cement and Concrete Research*, vol. 42, no. 2, pp. 377–383, 2012.

[33] K. Maekawa, T. Ishida, and T. Kishi, *Multi-Scale Modeling of Structural Concrete*, Taylor & Francis, New York, 1st edition, 2009.

[34] J. Xing, Y. Zhao, J. Qiu, and X. Sun, "Microstructural and mechanical properties of alkali activated materials from two types of blast furnace slags," *Materials*, vol. 12, no. 13, Article ID 2089, 2019.

[35] Q. Fu, M. Bu, Z. Zhang, W. Xu, Q. Yuan, and D. Niu, "Hydration characteristics and microstructure of alkali-activated slag concrete: a review," *Engineering*, vol. 20, pp. 162–179, 2023.

[36] J. Zhang, F. Zheng, Z. Liu, S. Hong, B. Dong, and F. Xing, "Nondestructive monitoring on hydration behavior of cement pastes via the electrochemical impedance spectroscopy method," *Measurement*, vol. 185, Article ID 109884, 2021.

[37] S. A. Bernal, M. C. G. Juenger, X. Ke et al., "Characterization of supplementary cementitious materials by thermal analysis," *Materials and Structures*, vol. 50, no. 1, Article ID 26, 2017.

[38] S. Adu-Amankwah, M. Zajac, C. Stabler, B. Lothenbach, and L. Black, "Influence of limestone on the hydration of ternary slag cements," *Cement and Concrete Research*, vol. 100, pp. 96–109, 2017.

[39] P. T. Durdziński, M. B. Haha, M. Zajac, and K. L. Scrivener, "Phase assemblage of composite cements," *Cement and Concrete Research*, vol. 99, pp. 172–182, 2017.

[40] M. Hlobil, V. Šmilauer, and G. Chanvillard, "Micromechanical multiscale fracture model for compressive strength of blended cement pastes," *Cement and Concrete Research*, vol. 83, pp. 188–202, 2016.

[41] C. Çetin, S. T. Erdoğan, and M. Tokyay, "Effect of particle size and slag content on the early hydration of interground blended cements," *Cement and Concrete Composites*, vol. 67, pp. 39–49, 2016.

[42] X.-Y. Wang, "Analysis of hydration kinetics and strength progress in cement-slag binary composites," *Journal of Building Engineering*, vol. 35, Article ID 101810, 2021.

[43] X. Feng, E. J. Garboczi, D. P. Bentz, P. E. Stutzman, and T. O. Mason, "Estimation of the degree of hydration of blended cement pastes by a scanning electron microscope point-counting procedure," *Cement and Concrete Research*, vol. 34, no. 10, pp. 1787–1793, 2004.

[44] T. Saeki and P. J. M. Monteiro, "A model to predict the amount of calcium hydroxide in concrete containing mineral admixtures," *Cement and Concrete Research*, vol. 35, no. 10, pp. 1914–1921, 2005.

[45] S. Mengxiao, W. Qiang, and Z. Zhikai, "Comparison of the properties between high-volume fly ash concrete and high-volume steel slag concrete under temperature matching curing condition," *Construction and Building Materials*, vol. 98, pp. 649–655, 2015.

[46] J. Ahmad, K. J. Kontoleon, A. Majdi et al., "A comprehensive review on the ground granulated blast furnace slag (GGBS) in concrete production," *Sustainability*, vol. 14, no. 14, Article ID 8783, 2022.